NAVY DEPARTMENT

DAVID TAYLOR MODEL BASIN

HYDROMECHANICS

AERODYNAMICS

STRUCTURAL MECHANICS

APPLIED MATHEMATICS

EXPERIMENTAL AND THEORETICAL STUDIES OF HYDROFOIL CONFIGURATIONS IN REGULAR WAVES

by

CDR Patrick Leehey, USN, and John M. Steele, Jr.

HYDROMECHANICS LABORATORY

RESEARCH AND DEVELOPMENT REPORT

October 1957

Report 1140

PRNC-TMB-648 (REV. 2-57)

EXPERIMENTAL AND THEORETICAL STUDIES OF HYDROFOIL CONFIGURATIONS IN REGULAR WAVES

by

CDR Patrick Leehey, USN
and John M. Steele, Jr.

October 1957

Report 1140
NS 500-002

TABLE OF CONTENTS

LIST OF ILLUSTRATIONS

LIST OF TABLES

NOTATIONS

a	Wave amplitude; wave height equals $2a$
C	Wave velocity
C, C_2, S, S_2	Coefficients of forcing functions
c	Lift coefficient
c'	Lift curve slope, $c' = \frac{\partial c}{\partial \alpha}$
D	Displacement of craft
d	Submergence of hydrofoil
F	Area of hydrofoil projected on horizontal plane
g	Acceleration of gravity
j	Longitudinal radius of gyration of craft
K, K', K_2, K_2'	Coefficients of displacement terms in equations of motion
k	Wave number $= \frac{2\pi}{\lambda}$
l	Horizontal distance from the center of pressure of a hydrofoil to the center of gravity of the craft
L	Lift of hydrofoil
p	Mean hydrofoil chord times the number of fore (or aft) hydrofoils
q	Distance from moving wave probe to craft c.g.
r	Computer, or REAC, time; $r = 10t$
$sgn\ x$	Signum function; equals 1 for $x>0$, -1 for $x<0$, and 0 for $x=0$.
t	Real time
U_0	Arbitrary initial data input to computer
V	Speed of advance of craft
W, W', W_2, W_2'	Coefficients of velocity terms in equations of motion
x, z	Surge and heave coordinates, respectively
z'	Derivative of z with respect to computer time, $\frac{dz}{dr}$
$\dot{z}$	Derivative of z with respect to real time, $\frac{dz}{dt}$
z_m	Heave amplitude
z_w	Vertical component of wave motion
α	Angle of foil incidence in radians
λ	Wave length

μ	Dihedral angle of a foil
σ	Root of stability equation
ρ	Density of water
τ	True wave period
τ'	Wave period relative to moving carriage
ϕ	Phase angle
ψ	Angle of pitch
ψ_m	Pitch amplitude
ω	Wave frequency (circular)
ω_r	Frequency of wave encounter

NOTE: When suscripts f and a are used they relate symbols for the given quantities to the forward and after hydrofoils, respectively. The additional subscript "0" denotes the equilibrium value of a quantity, e.g., c_{f_0} means the design lift coefficient of the forward foil. The symbol Σ denotes summation of fore and aft quantities and where used obviates the need for f and a subscripts.

ABSTRACT

This report presents a comparison of the experimentally measured and theoretically predicted values of the heave and pitch responses of area stabilized hydrofoil configurations to regular waves and to transient pulses. The theoretical responses were computed from the equations given by Weinblum in "Approximate Theory of Heaving and Pitching of Hydrofoils in Regular Shallow Waves," TMB Report C-479. Curves of heave and pitch amplitude magnification and phase lag are given as functions of wavelength.

The approximate linearized theory is found to give a qualitatively correct prediction of resonance and orbital motion effects. The theoretical amplitude magnifications are greater than the measured ones for most conditions, particularly for heave in following seas. This is believed to be caused principally by the neglect of nonlinear terms in the equations of motion.

A Mid-foil can be used with a tandem Vee-foil to cancel heave response to following seas of wavelength approximately equal to the outer foil spacing.

INTRODUCTION

In the design of modern hydrofoil craft, it is essential that the designer have information available on the responses of a proposed hydrofoil configuration to a given seaway. A linearized theory has been developed by Weinblum[1] which predicts the responses of a hydrofoil craft to regular waves. In order to determine the range of applicability of this theory, the heave and pitch of three area-stabilized hydrofoil configurations were measured in regular waves and compared with the heave and pitch predicted by the theory.

The experimental program consisted of taking continuous records of heave, pitch, wave form, and speed as the various configurations were towed through head and following waves in a towing tank. Transient response records and motion pictures of craft performance were taken. In addition, the craft parameters needed for determining the coefficients of the equations of motion were obtained experimentally.

Theoretical predictions of heave and pitch were obtained by solving the linearized equations of motion on the TMB Electronic Analog Computer. Experimental and theoretical responses were then compared by plotting heave and pitch amplitude magnifications and heave and pitch phase lags as functions of wave length.

This report is part of a general investigation of hydrofoil stability authorized in January 1955 by the Chief of the Bureau of Ships and carried out at the David Taylor Model Basin under Research and Development Project NS 500-002.

---

[1]References are listed on page 36.

EXPERIMENTAL EQUIPMENT

THE CRAFT

The hydrofoil craft used in these experiments is shown with its towing arm in Figure 1. The mass of the craft hull is simulated by an aluminum frame on which movable weights are mounted. These weights are used to balance the craft about its c.g. and to adjust its longitudinal radius of gyration. The foils can be mounted on the frame at several different positions. An axle is placed at the c.g. of the craft to which the towing arm is attached, thus allowing the craft to pitch freely about its c.g. Freedom in heave is obtained by attaching the towing arm to the carriage through another axle located at the c.g. of the towing arm. Since the towing arm is pivoted about its c.g. none of its weight bears on the craft. However, the inertia of the towing arm does affect the heave of the craft. The correction for this is discussed in in Appendix B.

The Wright 1903 airfoil section was chosen for the hydrofoils. The aerodynamic characteristics and offsets for this foil were obtained from Reference 2. This foil combines a steep lift curve with high angle of stall and small cross-sectional area. High lift was needed because of the relatively heavy craft that the foils were to support at a low flying speed, a high stall angle was needed to keep the foils operating well within the linear range of the lift curve at all times, and a small cross section was needed to keep the ratio of buoyant force to lift approximately the same as in full-scale hydrofoil craft. Three interchangeable foils were constructed, two identical 45 deg Vee-foils with 22 in. span and 2 in. chord and one flat foil with 12 1/2 in. span and 2 in. chord.

Three different craft configurations were tested. First, a configuration with identical Vee-foils fore and aft at equal distances from the c.g. which shall be called the Tandem Vee-foil Configuration. Second, a configuration with a Vee-foil forward and a flat foil aft equidistant from the c.g. which shall be called the Vee, Flat-foil Configuration. Third, a configuration similar to the Tandem Vee-foil Configuration except with a flat foil placed slightly forward of the c.g., this shall be called the Flat Mid-foil Configuration. Dimensions and properties of each configuration are given in Table 1, and photographs in Figures 2, 3, and 4.

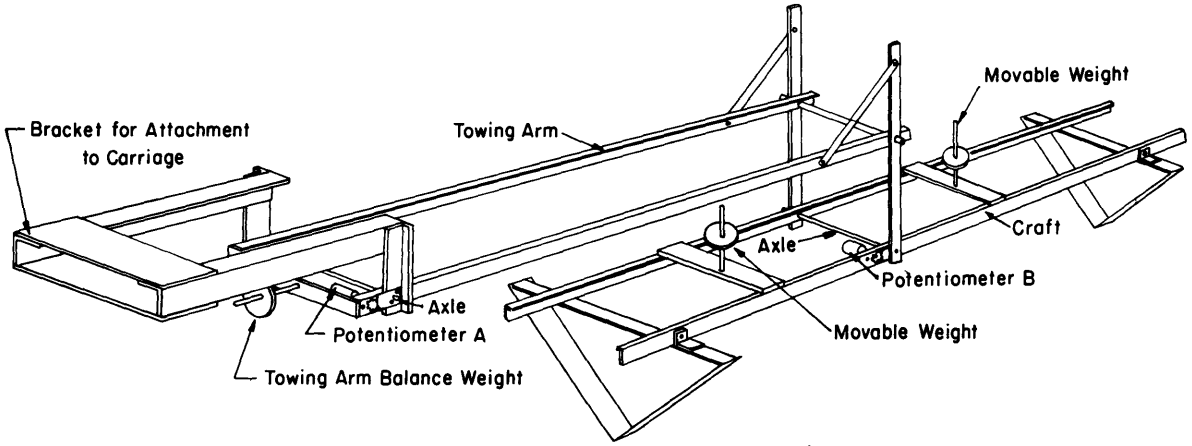

Figure 1 - Test Craft and Towing Arm

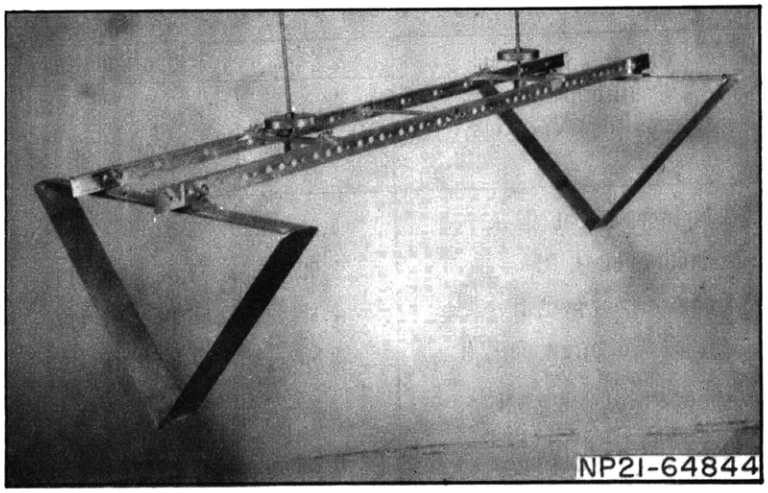

Figure 2 - Tandem Vee-Foil Configuration

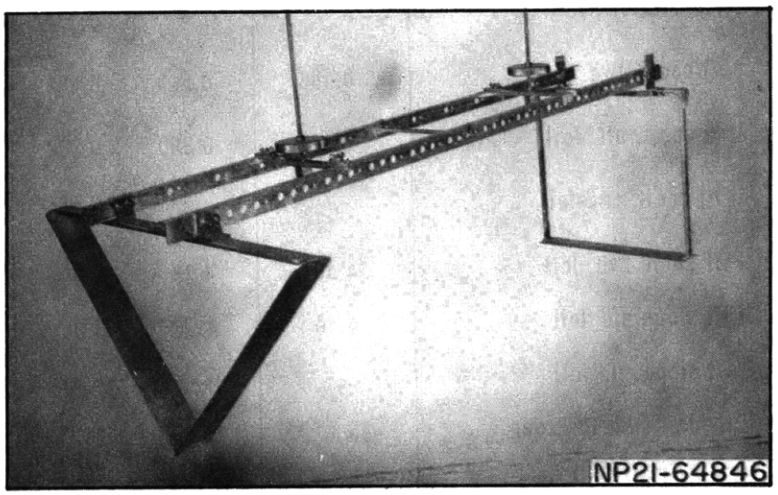

Figure 3 - Vee, Flat-Foil Configuration

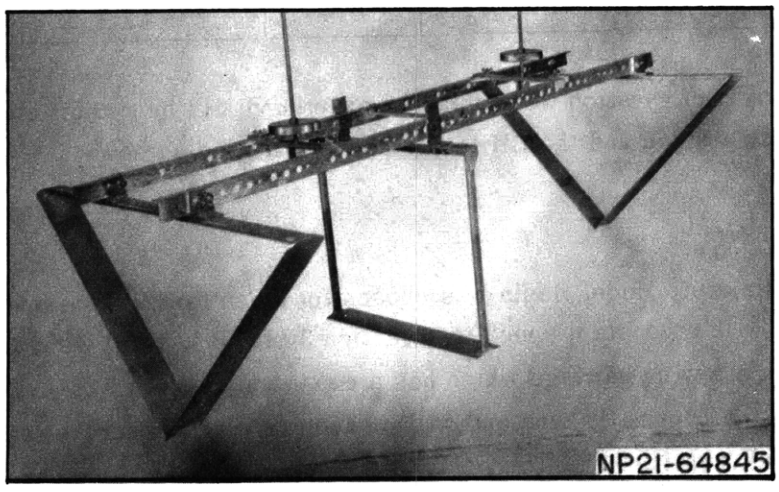

Figure 4 - Flat Mid-Foil Configuration

TABLE 1

Summary of Craft Characteristics

Symbol	Characteristics at Equilibrium flight condition; V ≈ 5 fps.	Configuration			
		Tandem Vee Foil	Vee, Flat Foil	Flat Mid-Foil	
				Head	Following
D	Displacement, lb	4.02	3.88	4.42	4.42
LOA	Length overall, ft	3.00	3.00	3.00	3.00
j	Long. rad. of gyr., ft	1.10	1.14	1.06	1.06
$l_f = l_a$	c.g. to fwd. or aft foil, ft	1.50	1.50	1.50	1.50
l_m	Midfoil fwd. of c.g., ft	–	–	0.27	0.27
F_{f_0}	Area fwd. foil, ft^2	0.183	0.168	0.122	0.196
F_{a_0}	Area aft foil, ft^2	0.183	0.174	0.142	0.196
F_{m_0}	Area mid-foil, ft^2	–	–	0.174	0.174
c_{f_0}	Lift coeff. fwd. foil	0.486	0.510	0.400	0.500
c_{a_0}	Lift coeff. aft foil	0.425	0.390	0.300	0.270
c_{m_0}	Lift coeff. mid-foil	–	–	0.200	0.200
c_f'	Lift slope fwd. foil	4.40	4.23	3.69	4.50
c_a'	Lift slope aft foil	4.40	4.73	3.90	4.50
c_m'	Lift slope mid-foil	–	–	4.73	4.73
μ_f	Dihedral fwd. foil, deg	45	45	45	45
μ_a	Dihedral aft. foil, deg	45	0	45	45
μ_m	Dihedral mid-foil, deg	–	–	0	0
$p_f = p_a = p_m$	Foil chord, ft	0.167	0.167	0.167	0.167

The longitudinal radii of gyration were obtained experimentally by two different methods, the Torsional Pendulum Method and the Bifilar Method[3], with good agreement.

TEST BASIN

The TMB Miniature Model Basin was chosen for these tests. This basin is approximately 55 ft long, with a constant speed test section 30 ft long, 2.0 ft wide and 2.0 ft deep. It is equipped with a towing carriage which has a maximum speed of 8 fps. The wavemaker in this basin is of the pneumatic type and will produce regular sinusoidal waves to a height of 3 in. and a length of 5 ft.

MEASURING EQUIPMENT

Lift measurements were made with a strain-gage dynamometer. This dynamometer, when used with a Sanborn Model 67 Recorder provides a continuous lift versus time trace during the entire carriage run. The carriage speed is set approximately beforehand and recorded accurately during the run by an interrupter type speed recorder. Lift measurements taken with this equipment are estimated to be accurate within $\pm$ 5 percent.

The pitch and heave of the craft were measured by recording the change in electrical signal from two microtorque potentiometers located as shown in Figure 1. Potentiometer A was fixed to the towing arm and its shaft geared to a stationary bracket. The change in voltage at potentiometer A is thereby directly proportional to the angular movement of the towing arm. Multiplying the angular movement in radians by the distance from the towing arm pivot to the c.g. of the craft yields the vertical displacement or heave. Potentiometer B was fixed to the craft and its shaft geared to the towing arm. Thus, the change in signal caused by the rotation of potentiometer B was proportional to the rotation of the craft with respect to the towing arm. To record the angular movement of the craft with respect to a fixed reference, i.e., the pitch, it was necessary to subtract the signal of potentiometer A from that of potentiometer B. This was done electrically; a diagram of the wiring is shown in Figure 5. The signals from the potentiometers were amplified on Sanborn Model 67-300 DC amplifiers and recorded on two channels of a four channel Sanborn Model 67 Recorder.

The other two channels of the recorder were used for recording continuously the wave height and speed. Wave height was supplied directly to the recorder by the standard capacitance type wave height measuring device used at TMB.[4] Typical response records are shown in Figures 6 and 7.

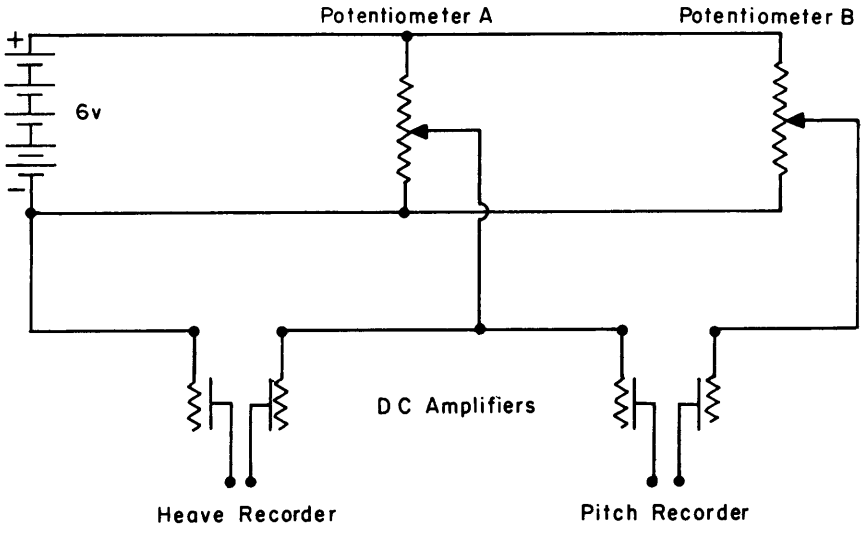

Figure 5 - Wiring Diagram for Recording Pitch and Heave

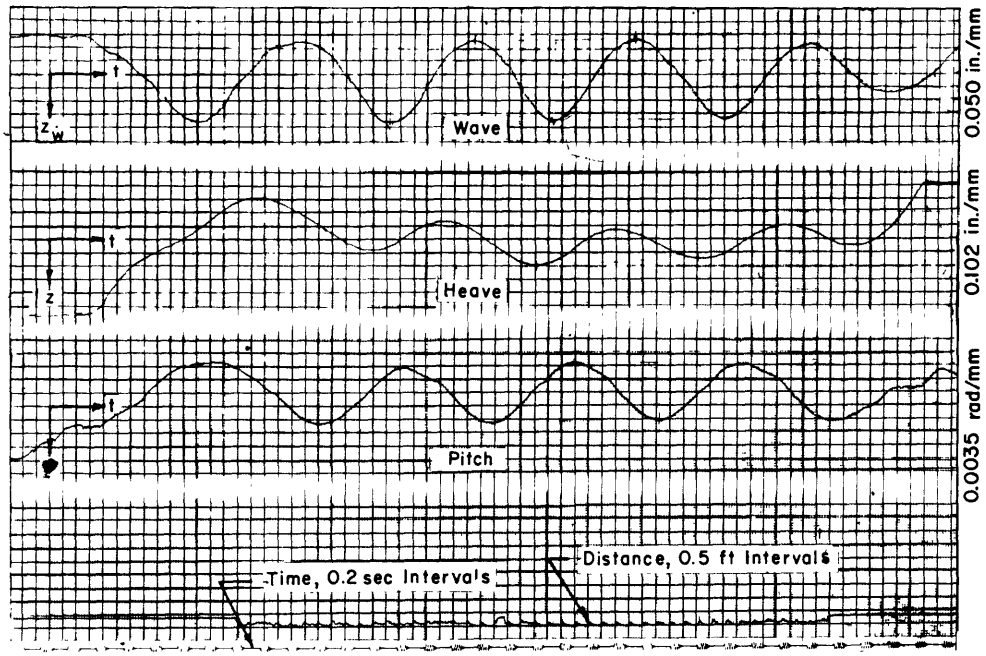

Figure 6 - Typical Following Sea Record, Tandem Vee-Foil Configuration
λ = 2.10 ft, 2a = 1.83 in., V = 5.0 fps

The microtorque potentiometers used were specified to be linear within 0.5 percent. They were calibrated in place by moving the craft through various combinations of pitch and heave and recording the deflections. The limits of accuracy of the various measurements are as follows: heave $\pm$ 0.02 in., pitch $\pm$ 0.05 deg, wave amplitude $\pm$ 0.01 in.

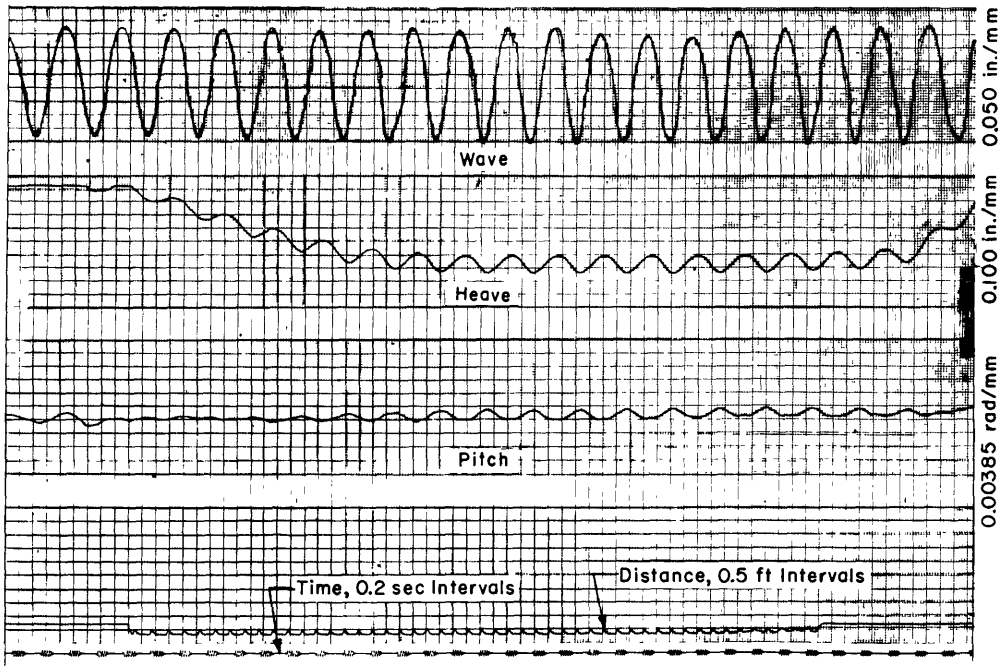

Figure 7 - Typical Head Sea Record, Tandem Vee-Foil Configuration
λ = 3.12 ft., 2a = 2.30 in., V = 5.0 fps

TESTS CONDUCTED

STEADY-STATE LIFT

In order to made theoretical computations of the craft's responses in waves it was necessary to obtain the steady-state lift characteristics of its foils. Lift data were taken on each foil at a carriage speed of approximately 5 fps for various angles of attack and several submergences. From these data the lift curves shown in Figures 8 and 9 were obtained. The three curves in Figure 8 show the effect of change of submergence (or aspect ratio) on the lift of the Vee-Foil. Since the theoretical maximum and minimum lift curve slopes are 2π and $\pi/4$ for infinite and zero aspect ratios respectively, lift curve slopes at other submergences can be obtained from a plot of slope versus aspect ratio as shown in Figure 10. No change in lift due to submergence was noted for the Flat-Foil until the submergence was approximately one chord length (2 in.) or less. Data taken at a 2 in. submergence is shown in Figure 9. In the stability tests, the Flat-Foil was never at a submergence less that 2.5 chords and consequently its lift curve was considered not to vary with submergence.

The steady-state downwash and the diving moment caused by drag were compensated for experimentally by adjusting the craft to fly at zero heave and trim in smooth water. No attempt was made to account for unsteady downwash effects.

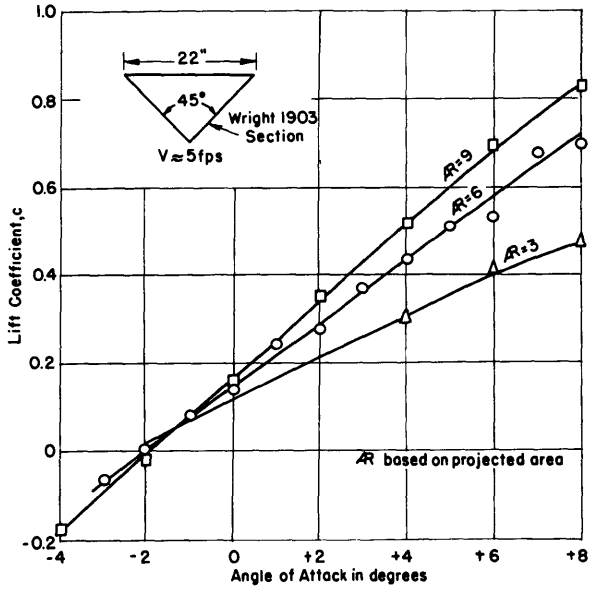

Figure 8 - Lift Coefficient versus Angle of Attack for Vee-Foil

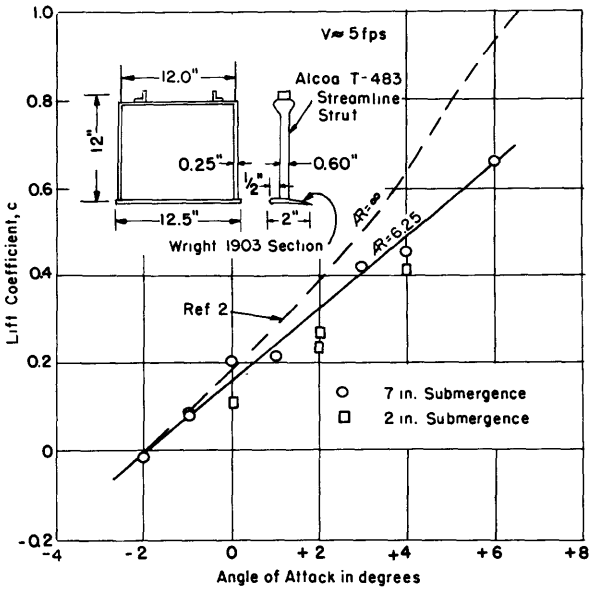

Figure 9 - Lift Coefficient versus Angle of Attack for Flat-Foil

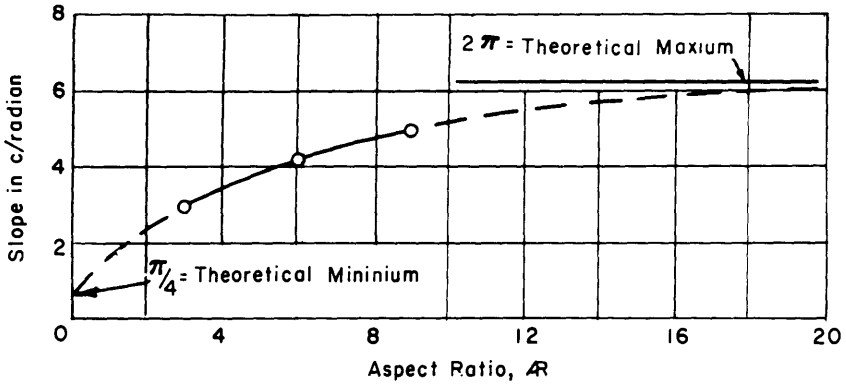

Figure 10 - Lift-Curve Slope versus Aspect Ratio for Vee-Foil

RESPONSES TO TRANSIENT PULSES

Tests were conducted on the Tandem Vee-Foil Configuration to determine its response, when flying in smooth water, to a sudden heave or pitch displacement. The displacement was imposed by pushing the craft downward after it had obtained its equilibrium flying conditions. The exact amounts of initial displacement and response were read from the record. The initial displacement and initial velocities of heave and pitch were used as initial data for the comparative theoretical solution. Results of these tests are shown along with the corresponding theoretical transients in Figures 11 and 12.

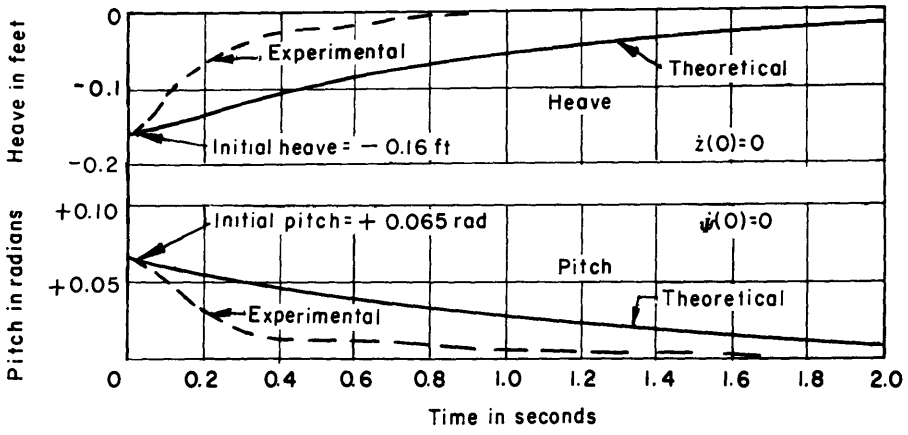

Figure 11 - Experimental and Theoretical Transient Responses of the Tandem Vee-Foil Configuration for Initial Heave and Pitch Displacements

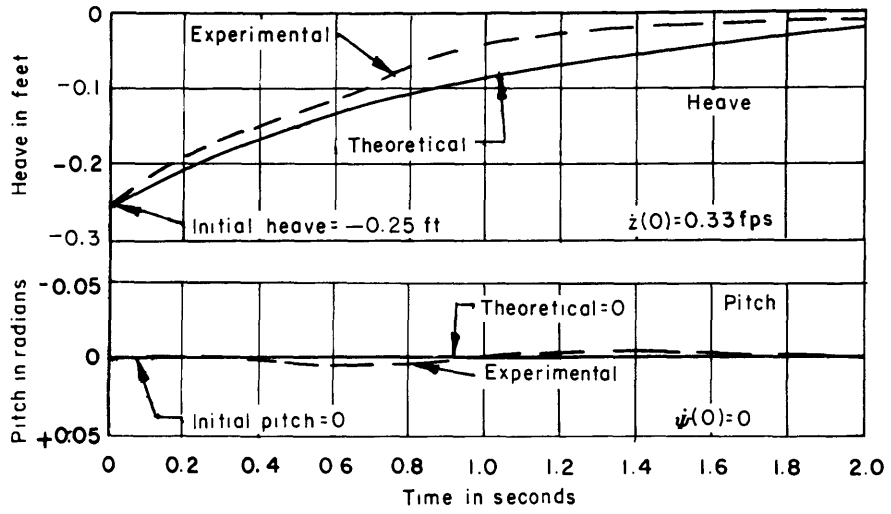

Figure 12 - Experimental and Theoretical Transient Responses of the Tandem Vee-Foil Configuration for an Initial Heave Displacement

RESPONSES TO REGULAR WAVES

Most of the testing consisted of recording the responses of the three configurations to various head and following waves. The maximum wavelength at which satisfactory records could be obtained was governed by the length of the basin. Due to the low frequency of encounter of the craft with the following waves, only waves of length 3 ft and under would produce at least one full response cycle of the craft. In head waves, waves of over 5 ft in length were reflected too quickly to obtain records free of reflected wave interference. Wave amplitudes were varied to a maximum of 1.13 inches. Typical oscillograph records are shown in Figures 6 and 7.

Essentially, four quantities were obtained from each record, heave amplitude magnification, pitch amplitude magnification, heave phase lag, and pitch phase lag. These are shown plotted against wave length in Figures 13 through 20.

The heave amplitude magnification factor is defined as z_m/a and is obtained from the records by dividing the amplitude of the heave trace by the amplitude of the wave-height trace and multiplying by a calibration factor. The pitch amplitude magnification factor is defined as $(\psi_m/a)\ l$ and is obtained similarly.

The heave phase lag is defined as the amount in degrees of wave cycle that the maximum upward craft heave lags the crest of the wave at the c.g. of the craft. The pitch phase lag is defined as the amount in degrees of wave cycle that the maximum upward craft trim lags the crest of the wave at the c.g. of the craft. Sample computations of heave, pitch, and heave and pitch phase lag from an experimental record are given in Appendix C.

MOTION PICTURES

Motion pictures were taken of the three configurations in head and following seas. The motion pictures are available from TMB, film No. M-1792. This film is considered a portion of the present report.

(Text continued on page 18.)

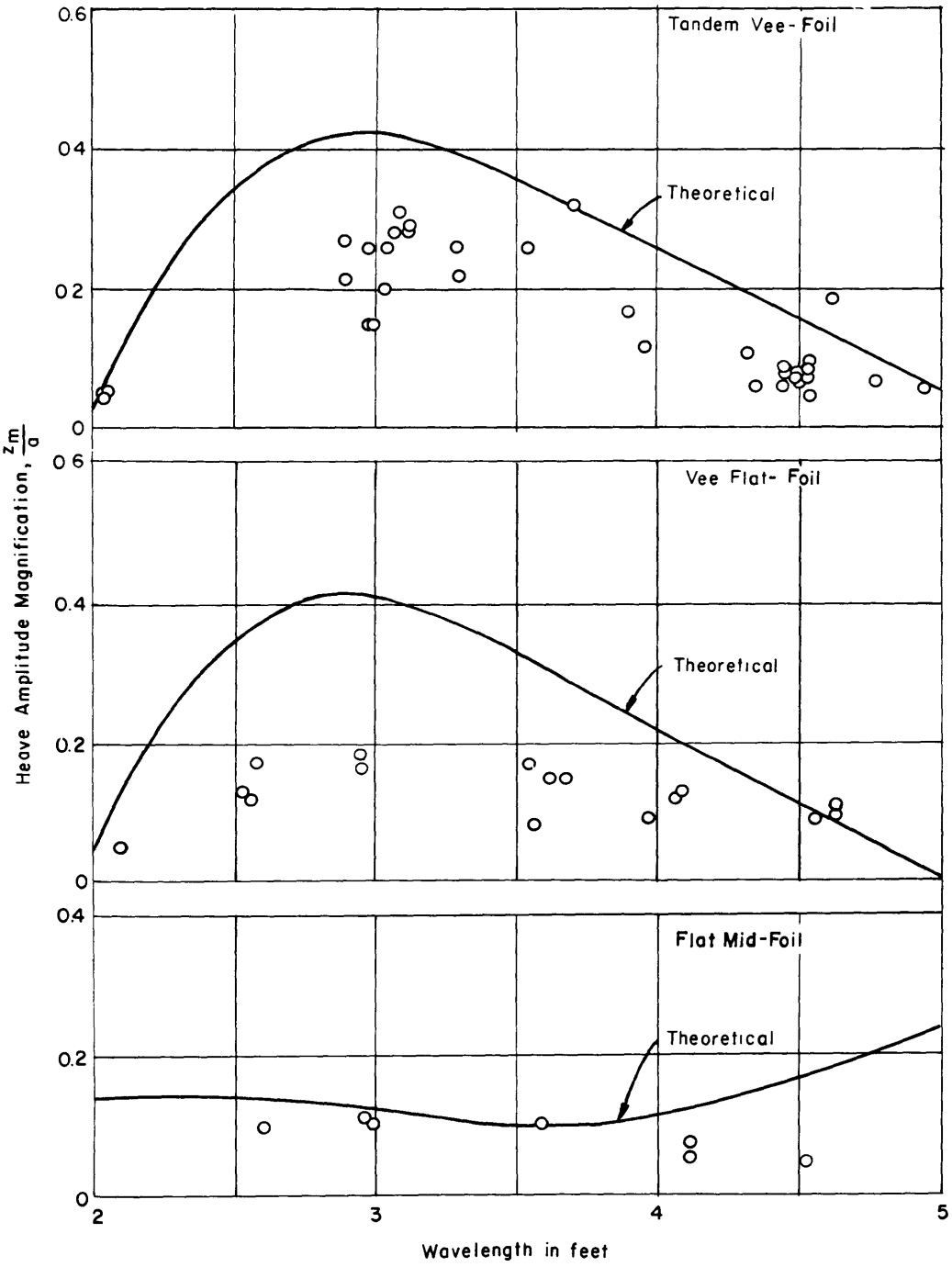

Figure 13 - Experimental and Theoretical Heave Amplitude Magnifications in Head Seas

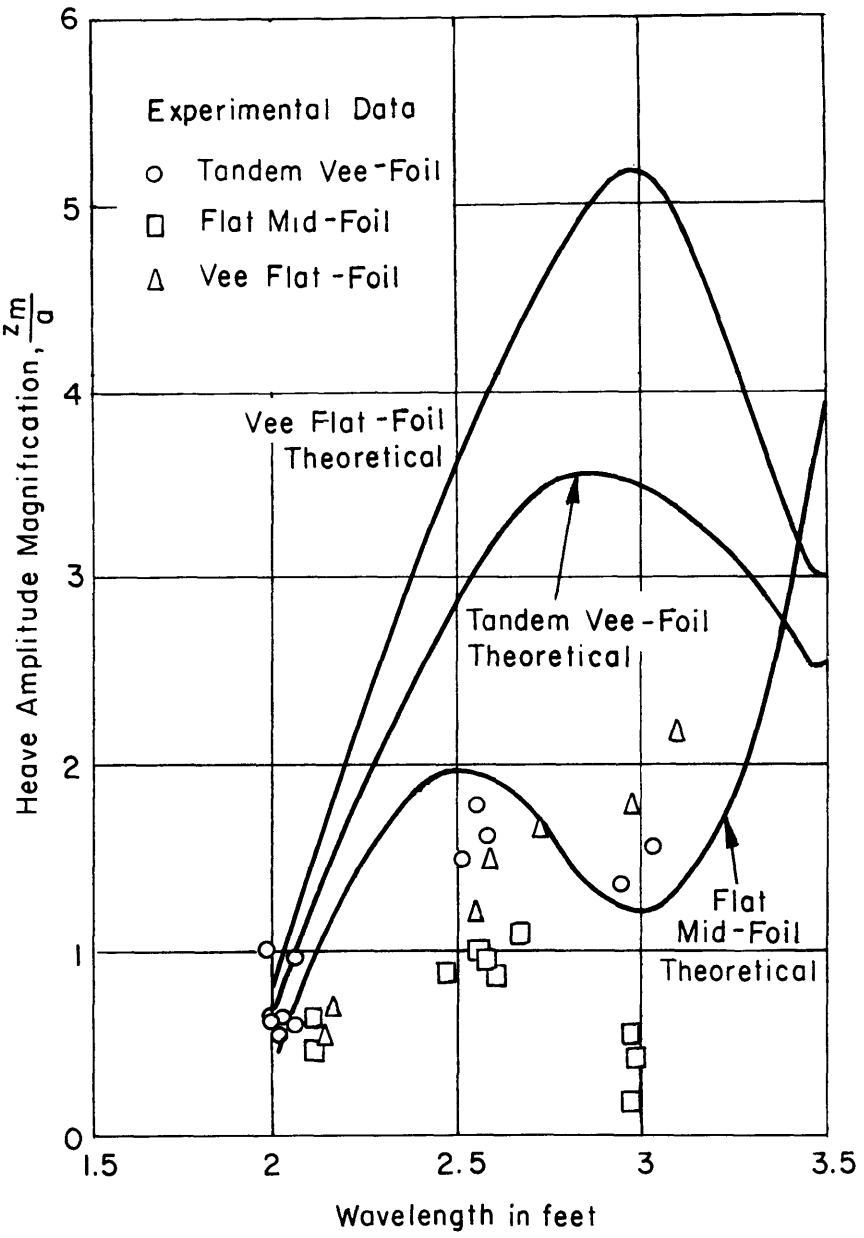

Figure 14 - Experimental and Theoretical Heave Amplitude Magnifications in Following Seas

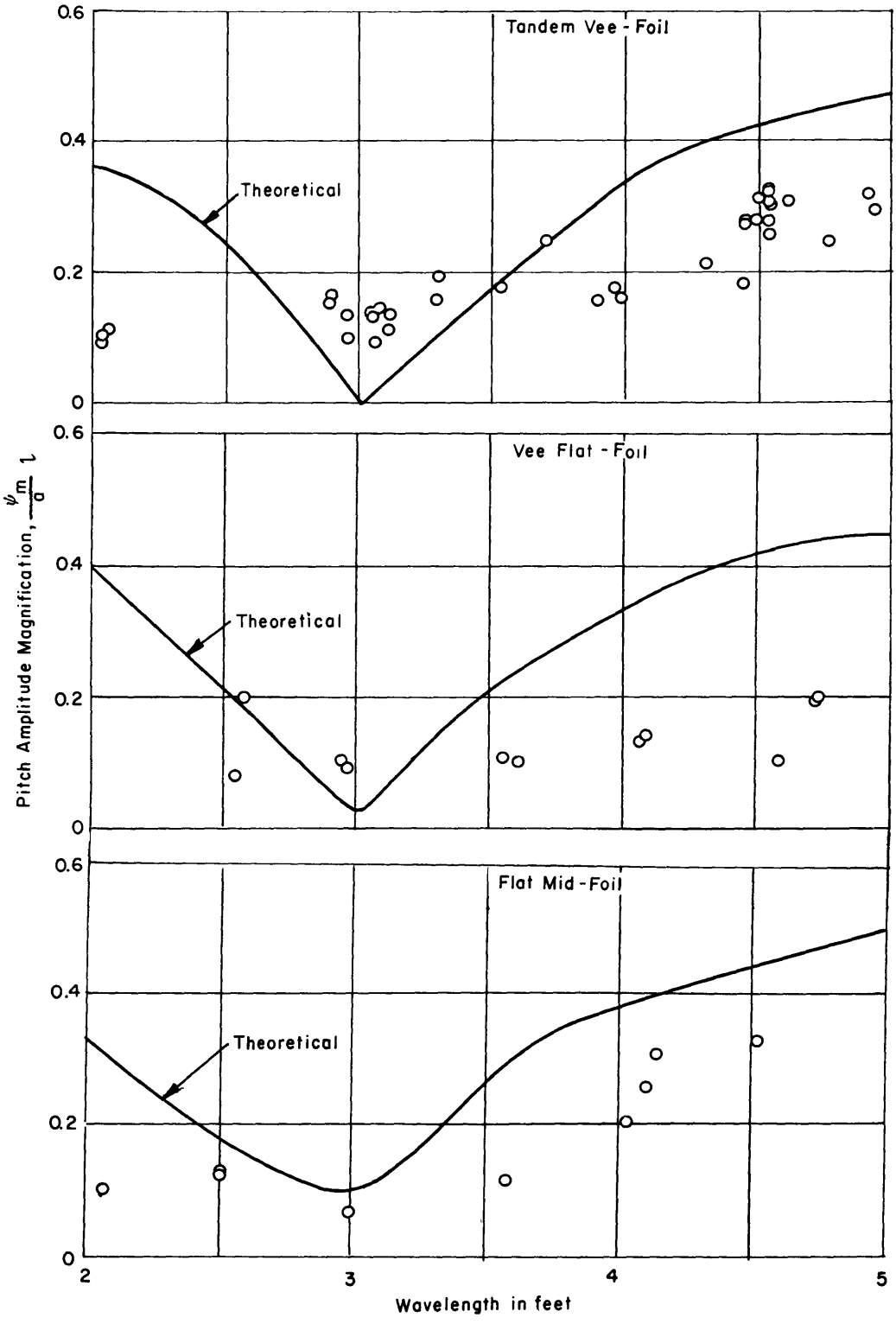

Figure 15 - Experimental and Theoretical Pitch Amplitude Magnifications in Head Seas

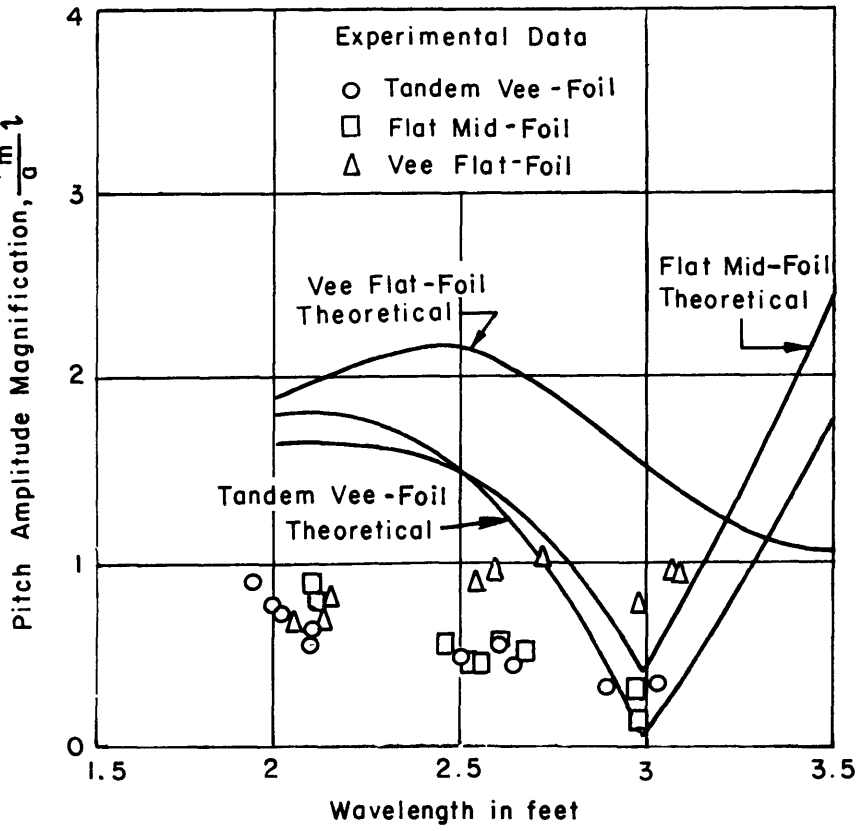

Figure 16 - Experimental and Theoretical Pitch Amplitude Magnifications in Following Seas

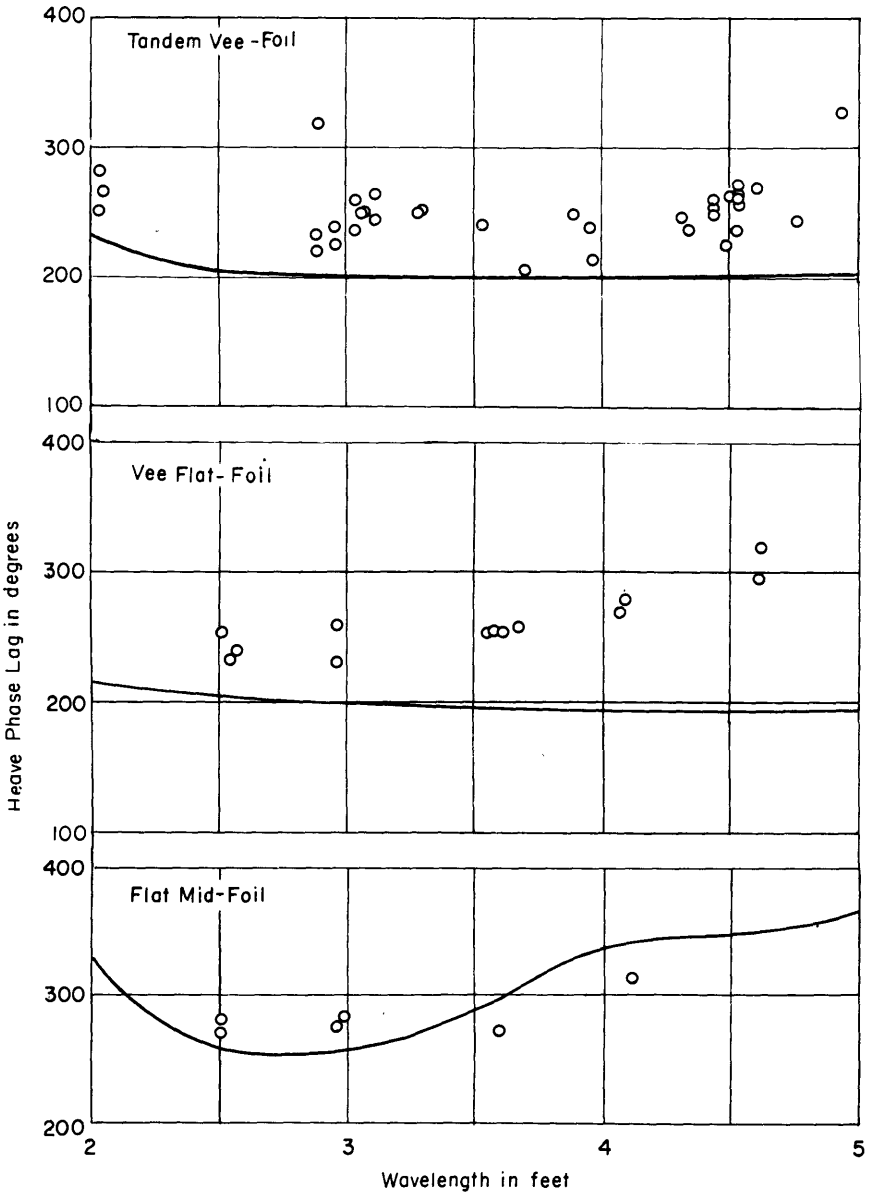

Figure 17 - Experimental and Theoretical Heave Phase Lag in Head Seas

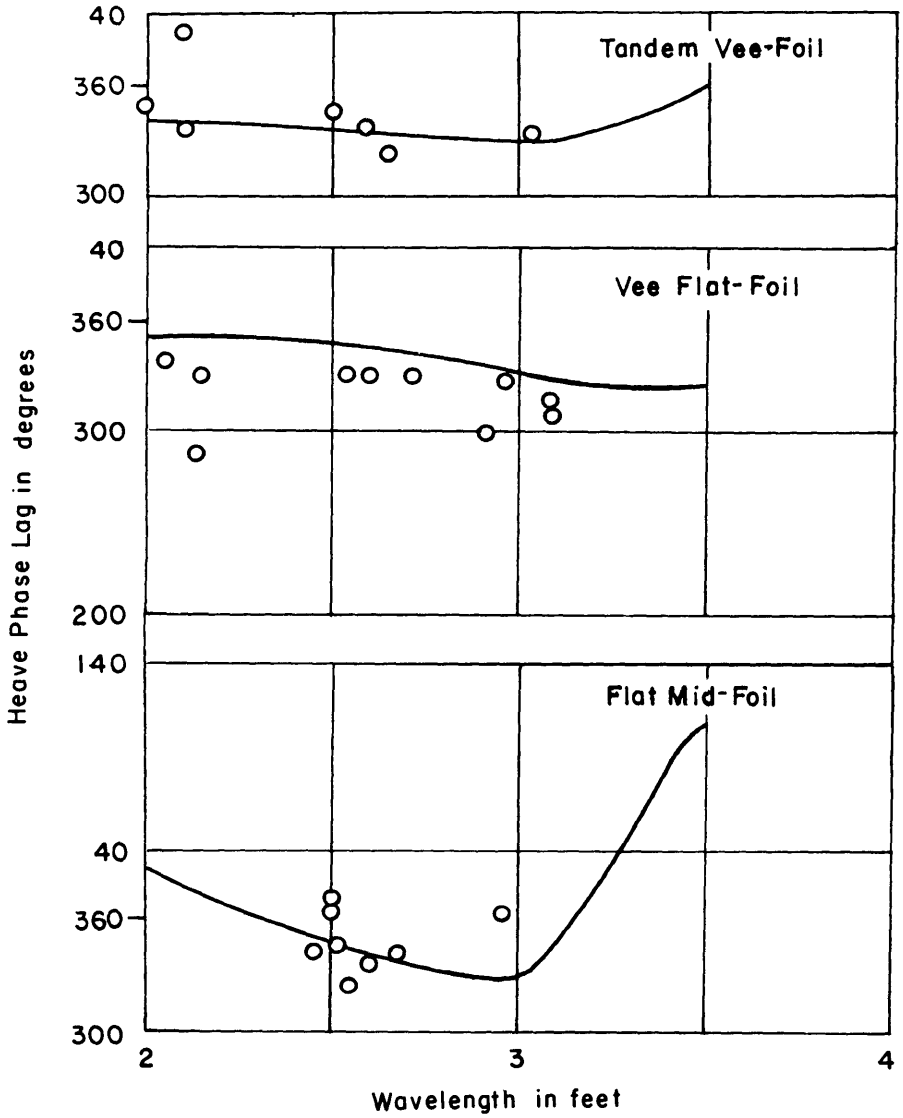

Figure 18.- Experimental and Theoretical Heave Phase Lag in Following Seas

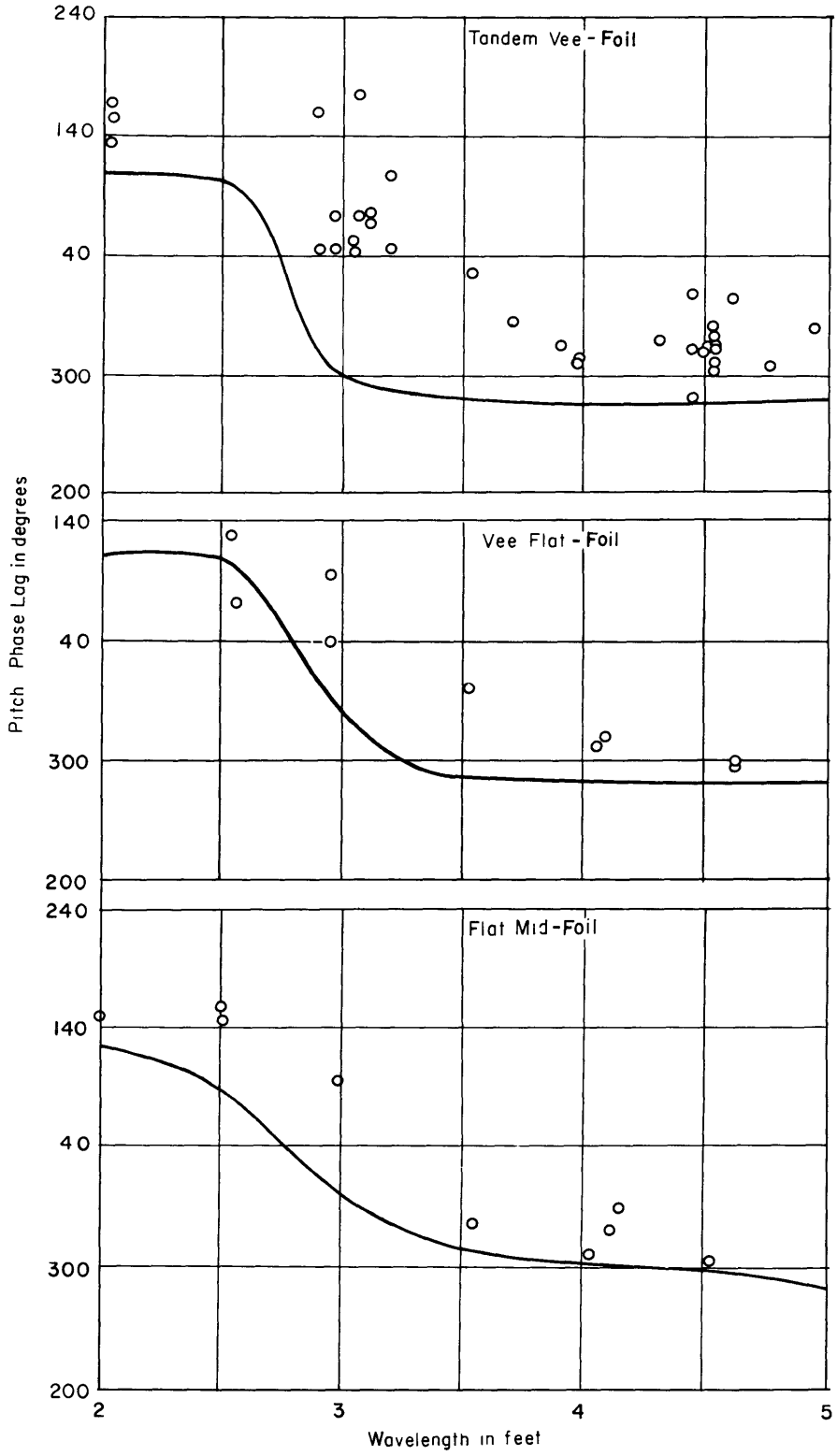

Figure 19 - Experimental and Theoretical Pitch Phase Lag in Head Seas

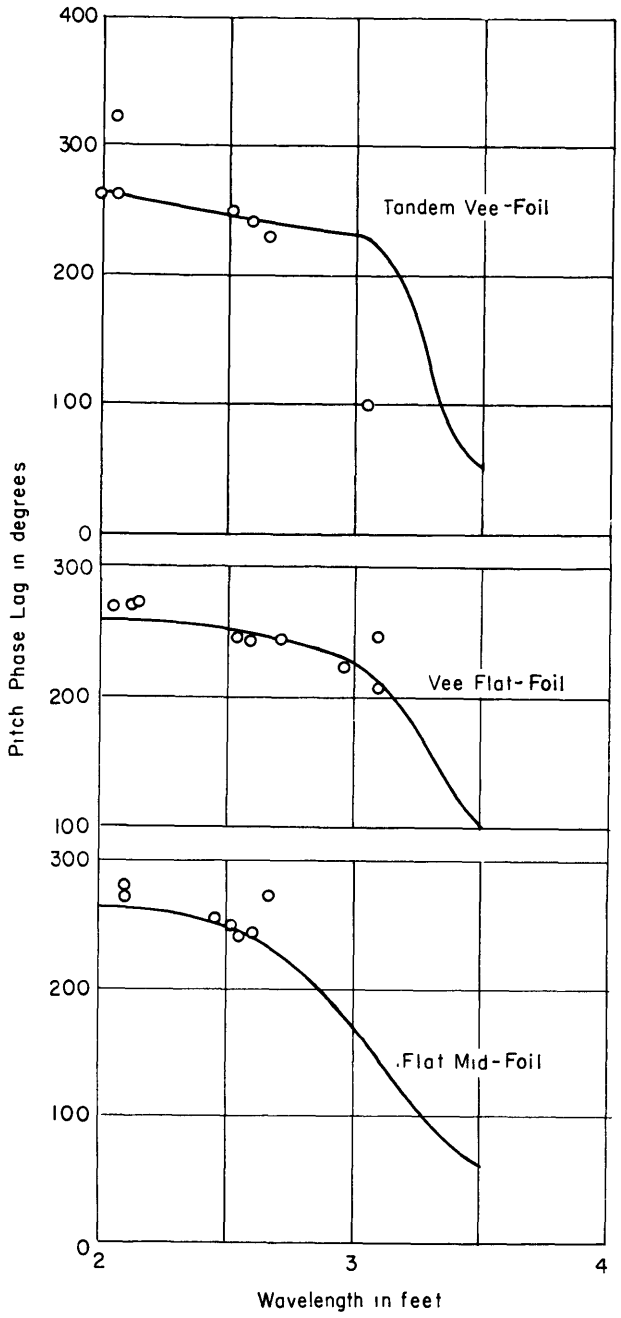

Figure 20 - Experimental and Theoretical Pitch Phase Lag in Following Seas

COMPUTATION OF THEORETICAL RESPONSES

EQUATIONS OF MOTION

Weinblum[1] expresses the longitudinal motion of an area-stabilized hydrofoil craft by a system of linear ordinary differential equations with constant coefficients.

$$\ddot{z} + W\dot{z} + Kz + W'\dot{\psi} + K'\psi = F(t)$$

$$\ddot{\psi} + W_2'\dot{\psi} + K_2'\psi + W_2\dot{z} + K_2 z = M(t)$$

for heave z and pitch ψ related to axes fixed at the c.g. of the craft. The forcing functions

$$F(t) = C\cos\omega_r t + S\sin\omega_r t$$

$$M(t) = C_2\cos\omega_r t + S_2\sin\omega_r t$$

represent the effect of flying through regular sinusoidal waves at a frequency of encounter ω_r. The coefficients of the left hand side terms of the heave and pitch equation are dependent solely upon craft characteristics in steady flight in smooth water. The coefficients of the right-hand side terms are rather complicated functions of both craft and wave parameters.

The coefficients were hand-computed for each configuration and for a range of wave lengths covering experimental conditions. The only modification made was a correction applied to the coefficients of the heave equation to compensate for the inertia of the towing arm of the experimental craft. This correction, and expressions for all of the coefficients are given in the appendices. Values of the left-hand side coefficients are summarized in Table 2 for each configuration at the 5 fps testing speed.

Table 2 - Summary of Coefficients of Equations of Motion

Coefficient		Configuration			
		Tandem Vee-Foil	Vee Flat-Foil	Flat Mid-Foil	
				Head	Following
Heave	W	+ 55.9	+ 57.6	+ 63.9	+ 90.9
	K	+ 52.6	+ 32.1	+ 41.0	+ 45.0
	W'	0	− 6.07	+ 1.90	+ 7.77
	K'	−200	−240	−310	−434
Pitch	W_2'	+118	+101	+ 71.6	+125
	K_2'	+110	+ 79.4	+ 73.3	+ 55.3
	W_2	0	− 4.70	+ 1.68	+ 6.88
	K_2	+ 4.90	+ 37.3	+ 7.78	+ 17.8

The craft did not attain exactly the same equilibrium conditions for each run, therefore mean values of foil area, lift coefficient, and lift slope were used for each configuration in order to minimize the theoretical computations. The equilibrium states attained by the Flat Mid-Foil Configuration in head and following seas were different enough to justify making separate theoretical computations for head and following seas. The craft properties given in Table 1 are those used in the computations of the left-hand side coefficients given in Table 2. Values of the right-hand side coefficients are shown as functions of wavelength in Figures 21, 22 and 23.

An inspection of the coefficients of the equations of motion given in Appendix A shows that the phase lag and the ratio of amplitudes of foil to wave motion must be independent of wave amplitude. A wave amplitude of 0.10 ft was used for convenience in the analog calculations.

RESPONSE TO REGULAR WAVES

The equations of motion were solved on the TMB Electronic Analog Computer. Figure 24 is a schematic circuit diagram for generating the forcing functions. The circuits for solution of the coupled heave and pitch equations are shown in Figure 25. The quantities z, ψ, z_w, (or ten or one hundred multiples thereof) were plotted on the automatic plotting table. From these curves the steady-state values of pitch and heave amplitude magnifications and pitch and heave phase lag were read. Solutions for several wavelengths for each configuration were hand computed using the method given by Weinblum.[1] The hand computed solutions agreed with the analog computer solutions with a maximum relative error of approximately 2 percent. Results of the theoretical steady-state responses are shown in Figures 13 through 20.

RESPONSES TO TRANSIENTS

Theoretical transient responses were also computed on the analog computer. In order to simulate a smooth water pulse test the forcing functions were disconnected and initial conditions were applied to z, $\dot{z}$, ψ, and $\dot{\psi}$. With a nonzero initial condition on either z, $\dot{z}$, ψ, or $\dot{\psi}$ curves of z and ψ were plotted. Thus, a set of four pitch and heave transients were obtained for a nonzero condition on each of the values z, $\dot{z}$, ψ, and $\dot{\psi}$. Since the equations of motion are linearized these curves can be added graphically, with appropriate factors, to obtain any set of initial conditions desired. The computed transient responses are shown in Figures 11 and 12.

STABILITY ROOTS

In an effort to determine whether or not the inherent stability of a configuration bore a significant relation to its response in a seaway, the roots of the stability quartic (see Appendix A) were computed for each configuration and are given in Table 3. These will be discussed in the next section.

(Text continued on page 25.)

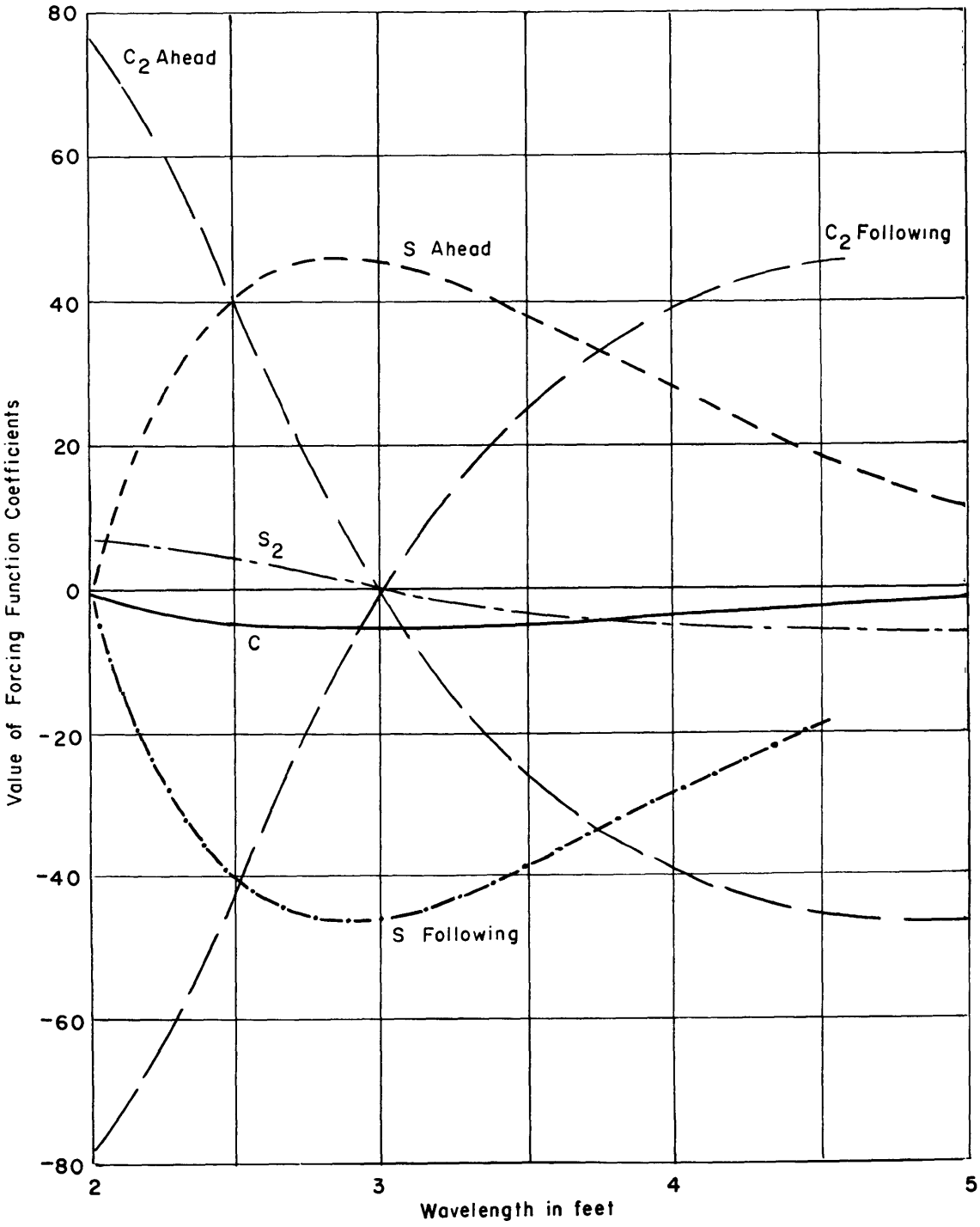

Figure 21 - Forcing Function Coefficients for the Tandem Vee-Foil Configuration

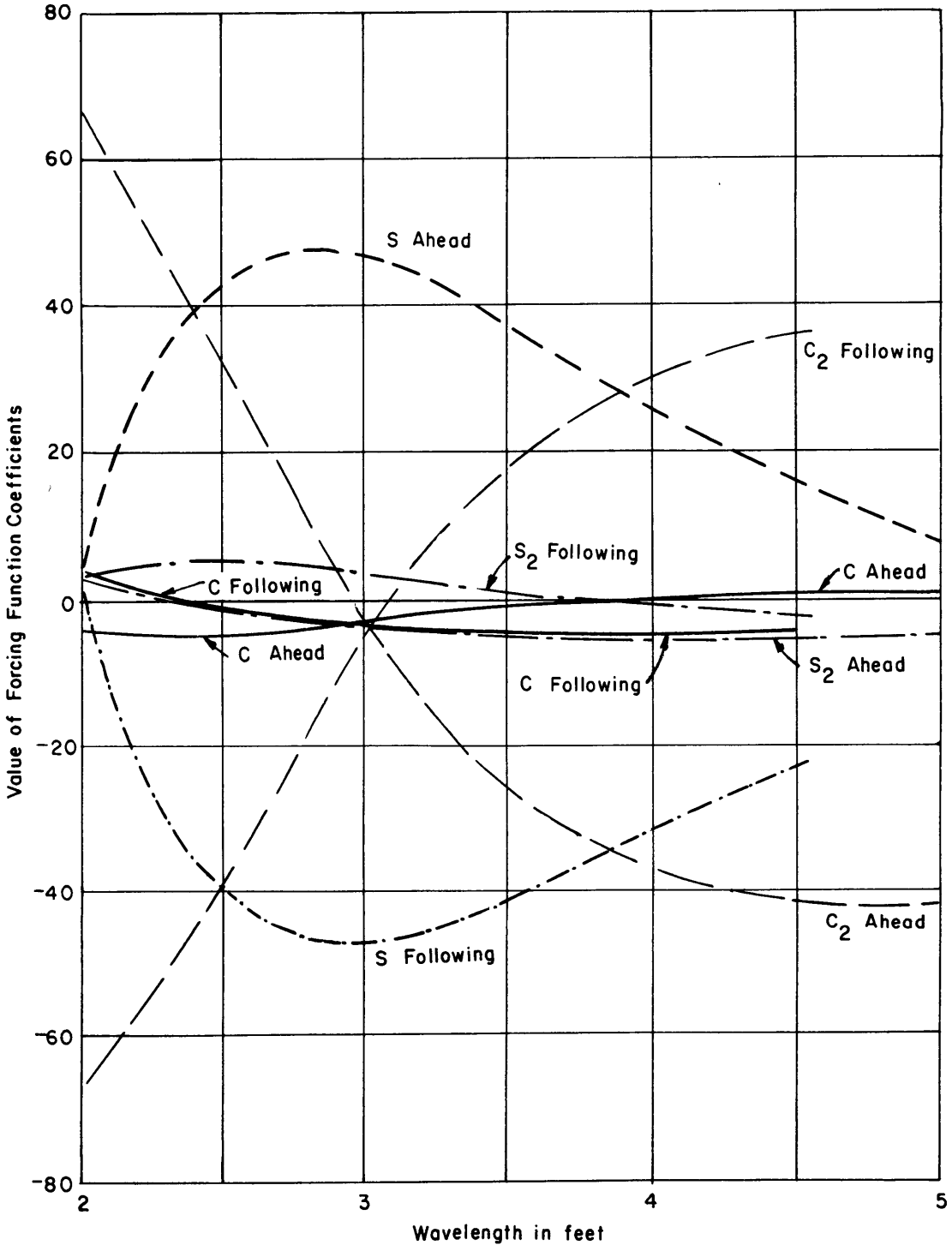

Figure 22 - Forcing Function Coefficients for the Vee, Flat-Foil Configuration

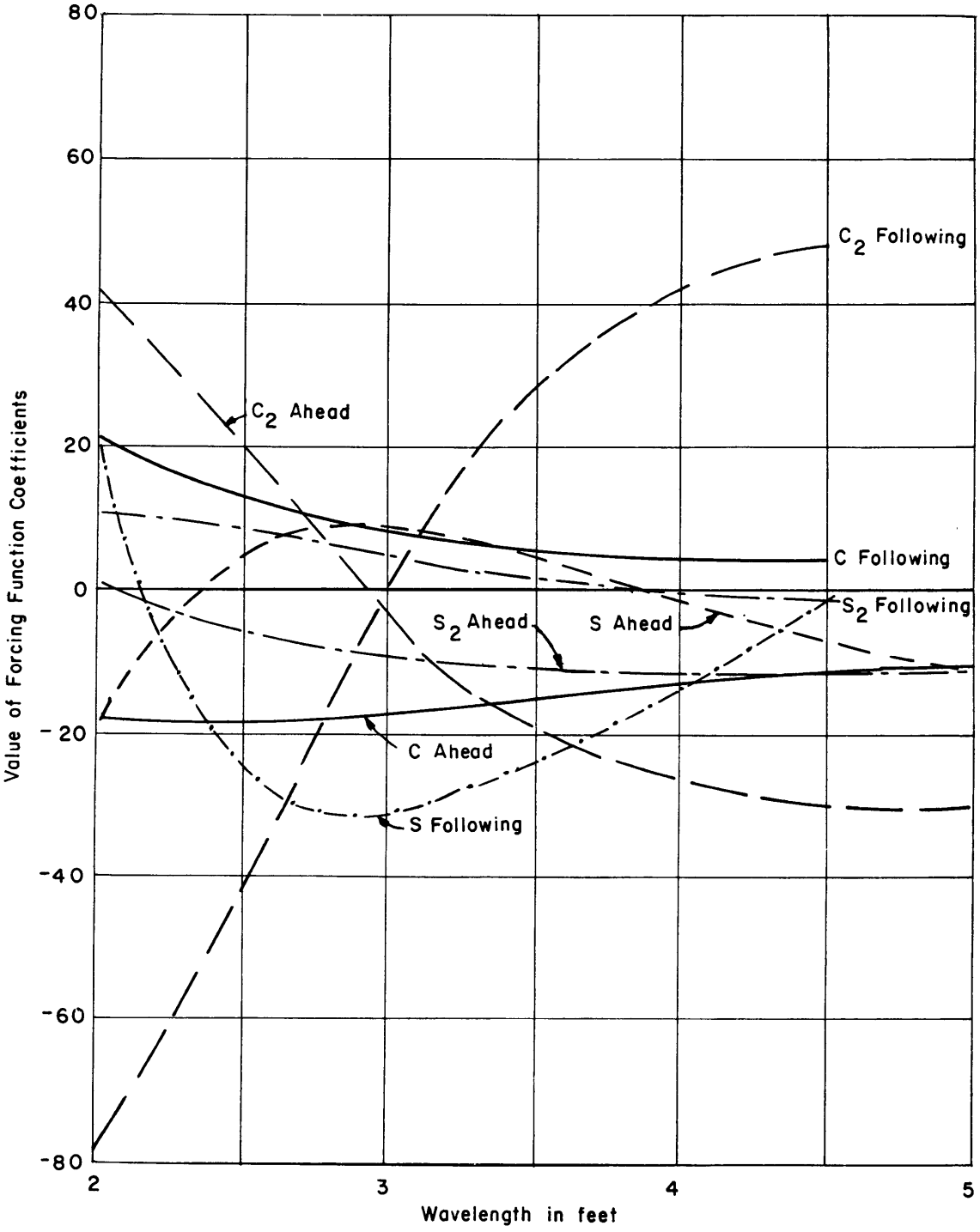

Figure 23 - Forcing Function Coefficients for the Flat Mid-Foil Configuration

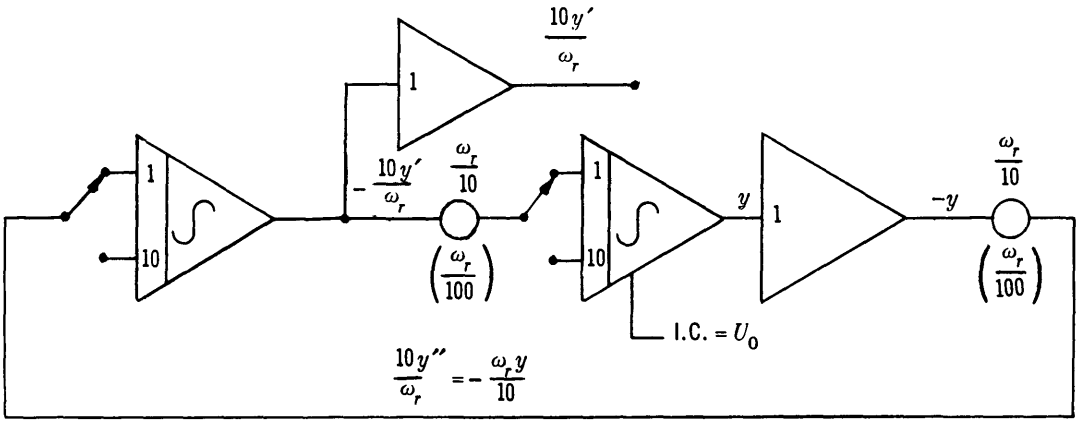

$$\tau = 10t$$

$$y = U_0 \cos \frac{\omega_r \tau}{10} \qquad y' = -\frac{\omega_r}{10} U_0 \sin \frac{\omega_r \tau}{10}$$

Note: alternative integrator gains and potentiometer settings are used for relative frequencies $\omega_r > 10$

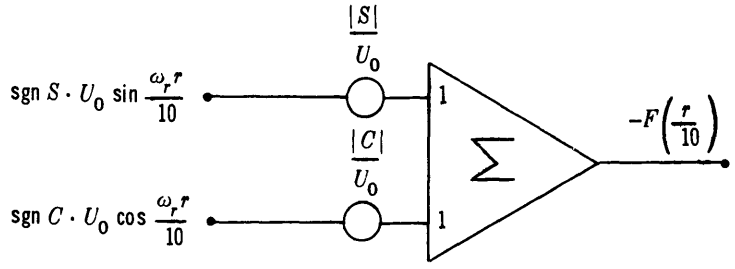

$$F\left(\frac{\tau}{10}\right) = C \cos \frac{\omega_r \tau}{10} + S \sin \frac{\omega_r \tau}{10}$$

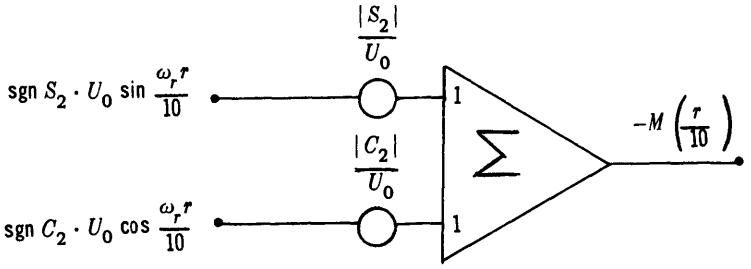

$$M\left(\frac{\tau}{10}\right) = C_2 \cos \frac{\omega_r \tau}{10} + S_2 \sin \frac{\omega_r \tau}{10}$$

Figure 24 - Analog Computer Diagram for the Generation of Forcing Functions

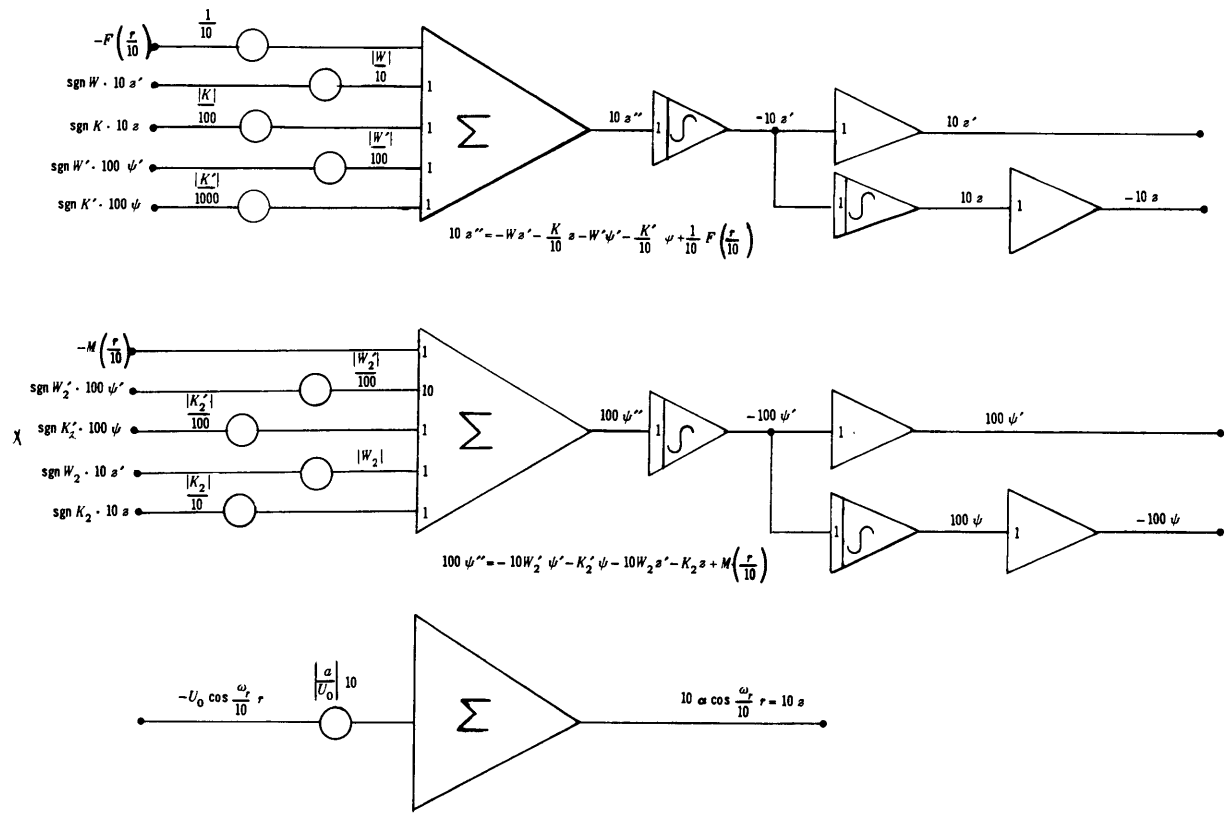

Figure 25 - Analog Computer Diagram for the Solution of the Coupled Pitch and Heave Equations

TABLE 3

Summary of Roots of Stability Equation

Root	Configuration			
	Tandem Vee-Foil	Vee Flat-Foil	Flat Mid-Foil	
			Head	Following
σ_1	- 116	- 100	- 71.6	- 127
σ_2	- 54.9	- 56.8	- 62.0	- 88.1
$Re\ \sigma_{3,4}$	- 0.950	- 0.578	- 0.900	- 0.596
$Im\ \sigma_{3,4}$	± 0.398	± 1.30	± 0.645	± 0.746

COMPARISON OF THEORETICAL AND EXPERIMENTAL RESULTS

RESPONSES TO TRANSIENTS

The equations of motion are particularly simple for the tandem Vee-foil configuration. For transient motions in smooth water one should expect (see column 1 in Table 3) the heave and pitch responses to small initial heave and pitch deflections and velocities to be heavily damped. In particular, since there is no heave coupling into the pitch equation, an initial pure heave deflection and velocity should result experimentally in essentially pure heave motion.

Two responses of the tandem Vee-foil configuration to initial transients are recorded. The transients were imposed simply by displacing the test craft by hand after it had attained equilibrium flying altitude (see TMB Film No. M-1792 for the motion picture record). Figure 11 shows the recorded response to initial heave and pitch deflections. It was possible to choose zero time at an instant when both heave and pitch velocities were zero. A comparison of these records with the theoretical transient motions obtained on the analog computer shows that the theoretical heave and pitch curves are of the same character as the experimental curves, e.g., no oscillations are present. It is evident, however, that the damping of the test craft in both pitch and heave is greater than the theory predicts.

Figure 12 shows the recorded response to initial heave deflection and velocity where, simultaneously, pitch deflection and velocity are essentially zero. As predicted by theory, pitch response is negligible. Again, the actual heave response is more highly damped than the theoretical response.

One concludes that the linearized motion equations give at least a qualitatively correct representation of the response of the configuration to small deviations from equilibrium flight in smooth water. The discrepancies which exist between the theoretical and experimental results well warrant a more thorough investigation than was possible within the scope of the present investigation. It is probable that they result from the neglect of either or both:

1. The apparent mass of the hydrofoils, or
2. the viscous damping effect of the water upon the hydrofoils.

A rough calculation of the apparent mass of the hydrofoils, resulting from their vertical acceleration indicates that it is of the same order of magnitude as the mass of the configuration.* It is therefore desirable to include this, and probably other unsteady flow effects, at least in the analysis of craft motion in head seas.

---

* This peculiar characteristic of the test craft results from its low flying speed and is not usually significant in full-scale craft.

RESPONSE TO REGULAR WAVES

Tandem Vee-Foil Configuration

From Figures 13 and 15 it is evident that in head seas the theoretical heave and pitch amplitude magnifications are greater than the experimental amplitude magnifications for nearly all wavelengths. The theoretical value of nearly zero pitch amplitude magnification when wavelength equals foil spacing (λ = 3 ft) is not attained experimentally. This is probably because of the unsteady downwash effect of the forward hydrofoil upon the after hydrofoil, a factor neglected in the approximate theory.

The experimental phase lag is somewhat greater than the theoretical phase lag in both heave and pitch in head seas (see Figures 17 and 19). There is considerable scatter in the data points. Phase lags are difficult quantities to determine accurately; one can show readily that small errors in measuring wavelength lead to appreciable errors in phase lag because of the effect of variations in wave velocity as computed from linearized wave theory. A direct means of measuring wave velocity would be desirable.

The experimental values of the pitch and heave amplitude magnifications are markedly less than the theoretical predictions for the tests conducted in following seas. The actual motions are, in fact, no longer small and consideration should be given in future investigations to the motion limiting effects of the quadratic terms neglected in setting up the equations of motion; see Reference 1, p. 19.

The theory predicts that the tandem Vee-foil configuration will not pitch in following seas of wavelength equal to foil spacing. Figure 16 indicates that, as in the case of the head sea, while zero pitch is not actually attained at λ = 3 ft, the pitch amplitude magnification decreases abruptly as this wavelength is approached. One notes further in Figures 18 and 20 that the theoretical and experimental heave and pitch phase lags agree remarkably well for following sea runs.

Vee and Flat-Foil Configuration

The remarks above are generally applicable to this configuration as well, except that pitch does not approach zero in following seas as λ approaches 3 ft, nor is such predicted theoretically.

This configuration differs from the previous one only in the use of a flat hydrofoil aft instead of a Vee-foil; load distribution and projected foil areas at equilibrium flight conditions remain essentially the same. The elimination of area-stabilization aft, however, reduces the heave and pitch stiffness coefficients K and K_2', respectively (cf. Table 2). This, in turn,

causes a reduction in the damping of the oscillatory mode of motion. Consequently, the Vee and flat-foil configuration shows larger heave and pitch amplitude magnifications in following seas than does the tandem Vee-configuration.

Flying this configuration through following seas of about 3.5 ft wavelength at 5 ft per second would produce an encounter frequency ω_r equal to the resonant frequency of the configuration. It is interesting to note, however, that maximum large heave and pitch amplitude magnification are not predicted by the approximate theory for this wavelength. The reason is that the coefficients of the forcing functions are themselves dependent upon the wavelength and are well below their peak values in a neighborhood of $\lambda = 3.5$ (see Figure 22).

Flat Mid-Foil Configuration

The performance of area-stabilized hydrofoil craft is much poorer in following seas than in head seas. This is due to two principal effects. One, that of resonance, has already been discussed. The other is the effect of the orbital particle motion of the waves. Briefly, the effect of this orbital motion is to increase the lift of a hydrofoil as it enters a head wave but to decrease the lift as it overtakes a following wave. Thus, in head seas added lift is obtained just when it is needed to carry the craft clear of a wave crest, while in following seas lift is partially destroyed just at the wrong time, sometimes resulting in a crash into a crest or a broach in a trough. In the equations of motion, the reversal of the orbital motion effect is indicated by the use of $\pm$ signs; see Appendix A and Reference 1.

Figure 14 shows large heave amplitude magnifications for both the tandem Vee-foil and Vee and Flat-foil configurations in following seas of wavelength equal to foil spacing (3ft in both cases). In contrast, heave amplitude magnifications in head seas at this wavelength are very small for both configurations – emphasizing the influence of orbital motion. It was reasoned that the detrimental effect of orbital motion in following seas could be alleviated for wavelengths near 3 ft by use of a third hydrofoil placed midway between the first two. The flat-foil was thus placed midway between the Vee-foils of the tandem configuration and angles of attack of the foils were adjusted to permit flight of this "mid-foil configuration" at nearly zero trim in smooth water. It was already evident that the original tandem Vee-foil configuration negotiated following 3-ft waves with negligible pitching motion (see Figure 16). Obviously, the fore and aft Vee-foils were being subjected simultaneously to the same orbital effects, generating a pure heave motion. The third hydrofoil at the half wavelength point would be influenced by a reversed orbital affect which would tend to cancel this heave. The experimental points on Figure 14 show dramatically that this is in fact the case. Curiously, the effect is more pronounced experimentally than it is theoretically; why this is so is not entirely clear.

The use of a third hydrofoil increased drag appreciably, especially in waves, and brought to light an effect which was perhaps masked in tests of the first two configurations. The drag in following waves is apparently greater than in head waves, necessitating an

increase in forward hydrofoil angle of attack for flight in following waves in order to counteract the increased drag moment about the center of gravity of the craft. This explains why two sets of coefficients and stability roots were calculated for this configuration.

In following seas of wavelength greater than 3 ft the craft would not maintain a constant mean attitude, but dived continually towards the water surface during a run. Similar behavior has been reported for full scale-craft operating in following seas. The whole matter deserves further attention; it may be that it will be necessary to make the forward hydrofoil of any area-stabilized configuration adjustable in angle of attack to allow in-flight correction of this difficulty.

CONCLUSIONS

Insight into the behavior of hydrofoil craft in waves can be obtained by correlating theoretically predicted motions with the results of tests of small models in a towing basin. Transient responses in smooth water and steady state responses to regular waves both show qualitative agreement with the solutions of linearized heave and pitch equations. However, the neglect of unsteady flow effect is apparent in head sea comparisons while the neglect of quadratic terms leads to exaggerated theoretical predictions of pitch and heave amplitude magnifications particularly in following seas.

The large pitch and heave amplitude magnifications experienced in following seas result from the combination of undesirable orbital motion effect upon hydrofoil lift together with a frequency of wave encounter near the resonant frequency of the configurations. In these waves, the amplitude magnifications are smaller for the tandem Vee-foil configuration than for the Vee and flat-foil configuration because of the inherently larger damping coefficient of the tandem Vee-foil configuration .

A mid-foil can be used with a tandem Vee-foil configuration effectively to cancel heave response to following seas of wavelength approximately equal to the outer foil spacing.

RECOMMENDATIONS FOR FURTHER RESEARCH

Unsteady flow, downwash, and quadratic term effects should be incorporated in the equations of motion and analog computer solutions obtained in order to obtain quantitatively correct comparisons with the experimental pitch and heave measurements.

Additional investigations of such devices as the mid-foil should be made in order to develop further means for limiting peak values of heave and pitch amplitude magnification in following seas.

The effect of increased drag and/or decreased lift in a seaway upon the mean flight path of hydrofoil configurations merits further investigation, particularly in following seas.

PERSONNEL AND ACKNOWLEDGMENTS

Mr. J.L. Power of the Fluid Dynamics Branch was responsible for establishing the design criteria for the test craft and towing apparatus, and for the major part of the preliminary planning of the experiment. Mr. G. Elkins of the Engineering Services Branch was responsible for the final design and working drawings of the test craft. The programming and initial computations of the theoretical responses on the TMB analog computer were done by the Motion Analysis Branch under Mr. J. Church. Mr. F. Ogilvie of the Ship-Wave Analysis Section assisted in the computation and checking of experimental and theoretical results.

APPENDIX A

WEINBLUM'S LINEARIZED EQUATIONS

For convenience of reference, Weinblum's linearized equations for the longitudinal motion of a hydrofoil craft in regular waves are presented.[1] Their derivation is based upon the assumption that heave, pitch, and wave amplitude are so small that all produce terms in these quantities and their derivatives may be neglected. Drag and thrust are assumed to retain equal magnitude but opposite sense along the same line of action while speed of advance remains constant through waves. Quasi-steady motion is assumed and the effect of forward foil downwash upon the lift of the after foil is neglected. The effect of the exponential decay of orbital motion with increasing submergence is assumed negligible.

The coupled linearized heave and pitch equations are

$$\ddot{z} + W\dot{z} + Kz + W'\dot{\psi} + K'\psi = F(t)$$

$$\ddot{\psi} + W_2'\dot{\psi} + K_2'\psi + W_2\dot{z} + K_2 z = M(t)$$

constant coefficients are determined from craft dimensions as:

$$W = \frac{g}{V}\frac{\Sigma c' F_0}{\Sigma c_0 F_0}$$

$$W' = \frac{g}{V}\frac{(c_f' F_{f_0} lf - c_a' F_{a_0} l_a)}{\Sigma c_0 F_0}$$

$$K = 2g\frac{\Sigma c_0 p \cot \mu}{\Sigma c_0 F_0}$$

$$K' = g\frac{2(c_{f_0} p_f l_f \cot \mu_f - c_{a_0} p_a l_a \cot \mu_a) - \Sigma c' F_0}{\Sigma c_0 F_0}$$

$$W_2' = \frac{g}{Vj^2}\frac{\Sigma c' F_0 l^2}{\Sigma c_0 F_0}$$

$$W_2 = \frac{g}{Vj^2}\frac{(c_f' F_{f_0} l_f - c_a' F_{a_0} l_a)}{\Sigma c_0 F_0}$$

$$K_2' = \frac{g}{j^2}\frac{2\Sigma c_0 p l^2 \cot \mu - (c_f' F_{f_0} l_f - c_a' F_{a_0} l_a)}{\Sigma c_0 F_0}$$

$$K_2 = \frac{2g}{j^2}\frac{(c_{f_0} p_f l_f \cot \mu_f - c_{a_0} p_a l_a \cot \mu_a)}{\Sigma c_0 F_0}$$

The periodic forcing functions imposed on the system by the regular waves are

$$F(t) = C \cos \omega_r t + S \sin \omega_r t$$

$$M(t) = C_2 \cos \omega_r t + S_2 \sin \omega_r t$$

In these equations the frequency of wave encounter is

$$\omega_r = \frac{2\pi}{\lambda} (V \pm C)$$

Where the positive sign applies to head seas and the negative sign applies to following seas. (It is assumed that wave velocity C does not exceed craft velocity V in following seas.) Retaining this sign convention the coefficients are

$$C = \frac{ag}{\Sigma c_0 F_0} \left[2 \Sigma c_0 p \cot \mu \cos kl \mp \frac{\omega}{V} (c_f' F_{f_0} \sin kl_f - c_a' \cdot F_{a_0} \sin kl_a) \right]$$

$$S = \frac{ag}{\Sigma c_0 F_0} \left[-2 (c_{f_0} p_f \cot \mu_f \sin kl_f - c_{a_0} p_a \cot \mu_a \sin kl_a) \mp \frac{\omega}{V} \Sigma c' F_0 \cos kl \right]$$

$$C_2 = \frac{ag}{j^2 \Sigma c_0 F_0} \left[2 (c_{f_0} l_f p_f \cot \mu_f \cos kl_f - c_{a_0} l_a p_a \cot \mu_a \cos kl_a) \mp \frac{\omega}{V} \Sigma c' F_0 l \sin kl \right]$$

$$S_2 = \frac{ag}{j^2 \Sigma c_0 F_0} \left[-2 \Sigma c_0 lp \cot \mu \sin kl \mp \frac{\omega}{V} (c_f' F_{f_0} l_f \cos kl_f - c_a' \cdot F_{a_0} l_a \cos kl_a) \right]$$

The stability equation is obtained by the classical procedure of assuming the existence of solutions to the homogeneous form of the equations of motion of the type $e^{\sigma t}$. This leads to the requirement

$$\sigma^4 + a\,\sigma^3 + b\,\sigma^2 + c\,\sigma + d = 0$$

where $a = W + W_2'$

$b = K + K_2' + W\,W_2' - W'W_2$

$c = KW_2' + WK_2' - K'W_2 - W'K_2$

$d = KK_2' - K'K_2$

If the roots of the above quartic equation all have negative real parts, any disturbances from steady-state flight will be damped exponentially and the corresponding configuration is called stable.

APPENDIX B

CORRECTION FOR INERTIA OF TOWING ARM

In this appendix the same notation as in Reference 1 is used except for the introduction of

l_T = distance from pivot of towing arm to c.g. of craft

I_T = moment of inertia of towing arm

I = moment of inertia of towing arm and craft about c.g. of towing arm

θ = angular displacement of towing arm about its pivot or c.g.

T = torque of towing arm about its c.g.

Neglecting drag forces on the craft,

$$T = (Z_1 + Z_2 - D)\, l_T$$

The vertical displacement of the craft is

$$z = l_T \theta$$

from which

$$\ddot{\theta} = \frac{\ddot{z}}{l_T}$$

Combining and utilizing $T = I\,\ddot{\theta}$ we have

$$(Z_1 + Z_2 - D)\, l_T^2 = \ddot{z}\left(I_T + \frac{D}{g}\, l_t^2\right)$$

Introducing $\frac{D}{g} = m'$ we have

$$-m'\ddot{z} + \left[\frac{m'}{m' + \frac{I_T}{l_T^2}}\right](Z_1 + Z_2 - D) = 0$$

which is identical to Equation 21 of Reference 1, from which

$$\ddot{z} + W\dot{z} + Kz + W'\dot{\psi} + K'\psi = F(t)$$

was derived, except for the factor $\left[\frac{m'}{m' + \frac{I_T}{l_T^2}}\right]$

Hence, it is evident from Reference 1 that by multiplying W, K, W', K', and $F(t)$ by

$$\left[\frac{m'}{m' + \frac{I_T}{l_T^2}}\right]$$

the effect of the inertia of the towing arm will be included in the computed craft responses.

APPENDIX C

SAMPLE CALCULATION OF HEAVE AND PITCH AMPLITUDE MAGNIFICATION AND HEAVE AND PITCH PHASE LAG FROM EXPERIMENTAL RECORDS

A following sea run will be described in detail and then the modification for the head sea runs will be shown. We will refer to the following sea run shown in Figure 6. The amplitudes of wave height, heave, and pitch are given by

$2a = k_1 \times$ (total amplitude of wave height record in *mm*) = 0.050 (36.5) = 1.83 in.

$2 z_m = k_2 \times$ (total amplitude of heave record in *mm*) = 0.102 (12) = 1.22 in.

$2 \psi_m = k_3 \times$ (total amplitude of pitch record in *mm*) = 0.00357 (21.4) = 0.0765 radians

from which the amplitude magnifications are computed as follows

$$\frac{z_m}{a} = \frac{1.22}{1.83} = 0.666$$

$$\frac{\psi_m}{a} l = \frac{0.0765}{1.83} \quad 18.0 \text{ in.} = 0.750$$

k_1, k_2, and k_3 are constants determined by calibration.

Since all of the waves in these tests can be considered deep-water waves, the wavelength is given by $\lambda = \frac{2\pi}{g} C^2$ where C, the wave velocity, can be determined from

$$C = \frac{-\tau' g + \sqrt{(\tau' g)^2 + 8\pi\tau' gV}}{4\pi}$$

τ' is the period of the wave trace and is read directly from the record, making use of the 1/5 second timing marks. The velocity of the craft is found from the record by comparing the 0.5 ft intervals on the distance trace with the timing marks. Thus, for this record, $\tau' = 1.20$ sec. $V = 5.00$ fps,

$$C = \frac{-1.20g + \sqrt{(1.20g)^2 + 8\pi (1.20)\ g\ 5.00}}{4\pi} = 3.28 \text{ fps}$$

and

$$\lambda = \frac{2\pi}{g} (3.28)^2 = 2.10 \text{ ft}$$

The wave probe was mounted a distance q ahead of the c.g. of the craft. Thus, in order to compare phase the wave trace must be shifted forward a time $t_c = \frac{q}{V - C}$ For the record under discussion

$$t_c = \frac{1.90}{5.00 - 3.28} = 1.10 \text{ sec}$$

When a peak of the wave trace is translated forward (in the direction of positive time) the time t_c, the phase lags are given by

$$\phi = \frac{d_l}{d_p} \; 360$$

Where d_l is the distance that a peak of a heave or a pitch trace lags the translated peak of the wave trace in time, and d_p is the distance corresponding to the periods of the heave, pitch, and wave traces. Thus, in this example

$$\phi_z = \frac{58mm}{60mm} \; 360 = 348 \text{ deg}$$

$$\phi_\psi = \frac{44mm}{60mm} \; 360 = 246 \text{ deg}$$

The head-sea records were analyzed similarly except that it was considered more accurate to obtain the wave period τ from a stationary wave probe. The wave velocity is then given by $C = \frac{\tau g}{2\pi}$. Also in head seas $t_c = \frac{g}{V + C}$.

REFERENCES

1. Weinblum, George P., "Approximate Theory of Heaving and Pitching of Hydrofoil in Regular Shallow Waves," David Taylor Model Basin Report C-479 (Oct 1954).

2. Loukianoff, G.S., "Tragflachen-Untersuchungen des aerodynamischen Laboratoriums der Technischen Hochschule Moskau," Zeitschrift fur Flugtechnik und Motorluftschiffahrt, 3, 153 (1912).

3. Barton, E.H., "Analytical Mechanics," Longmans, Green, and Co., London (1911), Sections 262 and 422.

4. Campbell, W.S., "An Electronic Wave-Height Measuring Apparatus," David Taylor Model Basin Report 859 (Oct 1953).

INITIAL DISTRIBUTION

Copies	
9	CHBUSHIPS, Tech Library (Code 312) 5 Tech Library 2 Prelim Design (Code 420) 2 Hull Design (Code 440)
1	CHBUAER, Res Div (RS-1)
3	CHONR 2 Mechanics Br (Code 438) 1 Amphibious Br (Code 465)
1	CHBUORD, SP 26
3	CNO 1 OEG (Op 03EG) 1 Amphibious Warfare (Op 343) 1 USW, R&D (Op 316)
1	DIR, USNRL
5	NAVSHIPYD BREM, Code 240
1	ASSTCOFS, G-3, USMC
1	COMDT, Marine Corps Schools Marine Corps Dev Ctr Quantico, Va.
1	Hdqrs, Air Res and Dev Comd Office of Scientific Res, Baltimore, Md.
1	USA Ord, Detroit Arsenal, Centerline, Mich. Attn: Head, Wheeled Vehicle Br
1	COMDT, USCG
2	DIR, Langley Aero Lab, Langley Field, Va. 1 Mr. J.B. Parkinson, Chief, Hydro Div
1	DIR, Aero Res, NACA, Wash, D.C.
1	DIR, Operations Res Office, Johns Hopkins Univ, Chevy Chase, Md.
1	DIR, Applied Physics Lab, Johns Hopkins Univ, Silver Spring, Md.
1	Document Services Ctr, ASTIA, Dayton, O.
1	Notre Dame Univ, Notre Dame, Ind. Dr. A.G. Strandhagen, School of Engin
2	CIT, Hydro Lab, Pasadena, Calif. 1 Dr. M.S. Plesset 1 Dr. T. Wu
1	Dr. L.G. Straub, Dir, St. Anthony Falls Hydro Lab, Univ of Minnesota, Minneapolis, Minn.
2	Institute for Math & Mech, New York Univ, New York, N.Y. 1 Dr. E. Bromberg 1 Dr. G. Morikawa
1	Dr. E. Wenk, Southwest Res Inst, San Antonio, Tex.
4	ETT SIT, Hoboken, N.J. 1 Dr. K.S.M. Davidson 1 Dr. Paul Kaplan 1 Dr. J.P. Breslin 1 Prof. B.V. Korvin-Kroukovsky

Copies	
3	Dept of Engin, Univ of California, Berkeley, Calif. 1 Prof. H.A. Schade 1 Dr. J.V. Wehausen 1 Dr. E.V. Laitone
1	Prof. M.A. Abkowitz, Dept NAME, MIT, Cambridge, Mass.
2	Iowa Inst of Hydraulic Res, St Univ of Iowa, Iowa City, Iowa 1 Dr. H. Rouse 1 Dr. L. Landweber
1	Univ of Maryland, College Park, Md. Prof J.B. Diaz
1	Editor, Appl Mech Reviews, c/o Southwest Res Inst, San Antonio, Tex.
1	Editor, Aero Engin Reviews, New York, N.Y.
1	Editor, Engin Index, New York, N.Y.
1	Grumman Aircraft Engin Corp, Bethpage, L.I., N.Y., Mr. W. Carl
1	Gibbs and Cox, Inc., New York, N.Y. Mr. M.G. Forrest
1	Baker Mfg. Co, Evansville, Wis. Mr. J.G. Baker
1	Miami Shipbldg Corp., Miami, Fla. Mr. R.J. Johnston
1	Ramo-Wooldridge Corp, Los Angeles, Calif. Dr. Rudolf X. Meyer
1	Mr. U.A. Pournaris, Rosenblatt & Sons, New York, N.Y.
1	Mr. J.D. Pierson, The Martin Co., Baltimore, Md.
8	ALUSNA, London
1	British Shipbldg Res Assn, London
1	Bassin d'Essais des Carenes, Paris, France
1	Canal de Experienceas Hidrodinamicas, Madrid, Spain
1	Nederlandsh Scheepsbouwkundig Proefstation, Wageningen, The Netherlands
1	Skipsmodelltanken, Trondheim, Norway
1	Statens Skeppsprovningsanstalt, Goteborg, Sweden
1	Dr. H. Lerbs, Hamburg Model Basin, Hamburg, Germany
1	Berlin Model Basin, Berlin, Germany
1	Laboratoire Dauphinous et Hydraulique, Neyrpic, Grenoble, France
1	Dr. G. Weinblum, Universitaet Hamburg, Hamburg Berliner Tor 21, Germany
1	Prof. Tetsuo Nishiyamo, Tohoku Univ, Sendai, Japan

NAVY-DPPO PRNC WASH D C